



OPEN

Closed-form solution of oscillating Maxwell nano-fluid with heat and mass transfer

Aamir Farooq^{1,2}, Sadique Rehman³, Abdulaziz N. Alharbi⁴, Muhammad Kamran⁵, Thongchai Botmart⁶✉ & Ilyas Khan⁷

The primary goal of this article is to analyze the oscillating behavior of Maxwell Nano-fluid with regard to heat and mass transfer. Due to high thermal conductivity of engine oil is taken as a base fluid and graphene Nano-particles are introduced in it. Coupled partial differential equations are used to model the governing equations. To evaluate the given differential equations, certain dimensionless factors and Laplace transformations are used. The analytical solution is obtained for temperature, concentration and velocity. The temperature and concentration gradient are also finds to analyze the rate of heat and mass transfer. As a special case, the solution for Newtonian fluid is discussed. Finally, the behaviors of various physical factors are studied graphically for both sine and cosine oscillation and give physical meanings to the parameters.

Abbreviations

T_{∞}	Ambient temperature (K)
g	Gravitational acceleration (ms^{-2})
β_m	Coefficient of thermal expansion (m^3/kg)
λ	Maxwell fluid parameter (s)
k	Thermal conductivity ($\text{Wm}^{-1} \text{K}^{-1}$)
ht	Heat transfer coefficient ($\text{Wm}^{-2} \text{K}^{-1}$)
ε	Space variable (m)
u	Velocity of fluid (ms^{-1})
Gr_m	Mass Grashof Number
r	Laplace parameter
C	Dimensionless concentration
nf	Nanofluid
μ_{nf}	Dynamic viscosity
q_r	Radiative heat flux
C_{∞}	Ambient concentration (kg/m^3)
β_t	Coefficient of thermal expansion (K^{-1})
ρ	Fluid density (kg m^3)
ν	Kinematic viscosity ($\text{m}^2 \text{s}^{-1}$)
c_p	Specific heat ($\text{J kg}^{-1} \text{K}^{-1}$)
t	Time (s)
θ	Dimensionless temperature
Gr_t	Thermal Grashof number
Rd	Radiation parameter
Pr	Prantl number
LT	Laplace transform
K	Chemical reaction parameter

¹Department of Mathematics, Zhejiang Normal University, Jinhua 321004, Zhejiang, China. ²Department of Mathematics, Abbottabad University of Science and Technology, Abbottabad, Pakistan. ³Department of Pure and Applied Mathematics, University of Haripur, Haripur, KPK, Pakistan. ⁴Department of Physics, College of Science, Taif University, P.O.Pox 11099, Taif 21944, Saudi Arabia. ⁵Department of Mathematics, COMSATS University Islamabad, Wah Campus, Islamabad 47040, Pakistan. ⁶Department of Mathematics, Faculty of Science, Khon Kaen University, Khon Kaen 40002, Thailand. ⁷Department of Mathematics, College of Science Al-Zulfi, Majmaah University, Al-Majmaah 11952, Saudi Arabia. ✉email: thongbo@kku.ac.th

hc Mass transfer coefficient
 M Diffusion specie coefficient

A large number of scientists and engineers are keen in knowing the computational and anatomical features of industrial fluid in recent times, because of their increasing usage in engineering and industrial sciences. Such fluids are categorized as non-Newtonian fluid, and their sub-division contains cement, drilling mud, synthetic oils, asphalts and many more¹. Some of the fluids show both the viscous and elastic properties such fluid are called viscoelastic fluids like toothpaste, polymers solutions, paints, clay etc.². The three major types of non-Newtonian fluids are Integral form, rate and differential type fluids. The Maxwell fluid is the principal viscoelastic rate type liquid, which is likewise broadly used. The differential structure and rate type models have stood out enough to be noticed among them. Due to the straightforwardness of rate type liquid, numerous examiners are giving specific consideration to Maxwell fluid^{3–6}. Riaz et al.^{7,8} studied the Maxwell fluid of heat and mass transport in term of local and non-local differential operators. The semi analytical solution was obtained via Laplace transform. A fractional Maxwell fluid was analyzed by^{9,10} using numerical techniques. Natural convection flow of Maxwell fluid between vertical plates was investigated by Na,W et al.¹¹. A closed- form solution was acquired through Laplace transform. Khan et al.^{12,13} studied mixed convection Maxwell fluid ordinary and fractionally over oscillating vertical plate. Exact solution and some special cases for Newtonian fluid was obtained through Laplace transform. Abro, K. A. et al.¹⁴ also obtained analytical solution of Maxwell fluid over vertical plane. Numerical solution of comparative Maxwell and Casson fluid was illustrated by Kumar et al.¹⁵ using Runge- Kutta based shooting method. Sodium alginate (SA-NaAlg) based (MoS2) nanofluid was researched by Ahmed et al.¹⁶ utilizing Maxwell Garnetts and Brinkman models. Physically, mixed convection is induced because of upgrade force and abrupt plate motion. Farooq et al.¹⁷ analyzed the generalized Maxwell model flow of magnetic hydrodynamic (MHD) fluid through porous duct. The solution was obtained via double Fourier sine and Laplace transform. Exact solutions for unsteady MHD flow of Maxwell fluid over oscillating plate have been illustrated by^{18,19}. Sandeep et al.²⁰ discussed the comparative study of Jeffery, Maxwell and Oldroyd-B fluid through extended surface utilizing similarity transformation and solution was acquired numerically via Runge–Kutta dependent shooting method. A fractional Maxwell model in porous medium was illustrated by Aman, S et al.²¹. The numerical solution was obtained using Stehfest's algorithm. Fetecau et al.²² studied the second problem of Stokes for Maxwell fluid via Laplace transform.

Coupled heat and mass transport is a process that happens commonly in nature. It exists not only as a result of temperature variations, but also because of concentration variations or the combine effect of these two. The impact of a compound response is dictated by, whether it is homogeneous or heterogeneous. The incorporation of unadulterated water and air, are inconceivable in nature. It's conceivable that any external matter is normally there, or that it's blended in with air or water. At the point when an external mass is available in air or fluids, it prompts a synthetic response. Numerous substance advances, like the assembling of pottery, the creation of polymers and food handling, benefits from the investigation of related synthetic responses. Shateyi²³ considered the Maxwell fluid on an extended sheet over Darcian medium. The general solution for natural convection flow past on a vertical plate with heat and mass transfer was discussed by^{24,25}. Free convection flow with heat and mass transfer over fluctuating and accelerated vertical plate through porous medium was studied by^{26–28}. Closed-form solution was obtained via Laplace transform method. Rajput et al.²⁹ researched the impact of radiation on an impulsively vertical plate with heat and mass transmission of MHD flow. Pattnaik, J. R et al.³⁰ addressed the MHD flow over exponentially inclined plate via porous medium. For solving the given equations Laplace transformation was utilized. Seth et al.³¹ illustrated the MHD convected flow of Soret and Hall effects in a rotating system with heat and mass transmission. Kumam, P et al.³² explained the comparative study of fractional Maxwell fluid. Semi analytical solution was obtained via Laplace transformation. Fetecau et al.³³ examine the impact of radiation and porosity on MHD fluid on an oscillating vertical layer. Tang et al.³⁴ have given the comparison of two different fractional definitions (Caputo, Caputo–Fabrizio) of Maxwell fluid.

Nanofluids are being used to improve the thermal conductivity of base fluids such as water, engine oil, propylene glycol, and ethylene glycol, among others. They have a wide range of uses in engineering and biomedicine including cooling, cancer treatment and industrial plants. The use of solid particles suspension to improve the thermal conductivity of traditional heat transfer fluid is a relatively new advancement in engineering technology. This technology has been recently paired with advance nanofluids and liquid nanoparticles suspensions technologies, to establish a new group of nanofluids based on solar collectors. Aman et al.³⁵ studied the natural convection flow of Maxwell fluid with graphene nanoparticles. Murtaza et al.³⁶ examined the concrete nanoparticles in fractional Maxwell fluid. Exact solution was acquired via LT. The Maxwell hybrid nano-fluid of convective flow in a channel was discussed by^{37,38}. Asjad et al.³⁹ investigated the clay-nanoparticles of generalized Maxwell fluid in heat transmission via infinite flat surface. Wang et al.⁴⁰ argued the Oldroyd-B nanofluid of MHD natural convection flow via permeable medium. Arif et al.⁴¹ studied the Maxwell hybrid nanofluid (engine oil) in vibratory vertical cylinder. Kumar et al.^{42,45} studied the impact of magnetic dipole on thermophoretic particle deposition in the flow of Maxwell fluid and nanofluid over a stretching sheet. Prasannakumara⁴³ focused on the numerical simulation of heat transport in Maxwell nanofluid flow over a stretching sheet considering magnetic dipole effect. Through the stretchable disks slip flow of Casson–Maxwell nanofluid was studied by Gowda et al.⁴⁴. Also, many other authors focused to studied Maxwell nanofluid, see e.g.^{46–48} for better understanding. Cheng et al.⁵⁰ proposed the heat transfer analysis of elastoviscoplastic non-Newtonian generalized fluid with hybrid nanofluid and dust particles. Numerical solution of the model is acquired via shooting method. Kaneez et al.^{51,52} investigated the numerical solution of micropolar fluid including dusty, mono and hybrid nono-structures. Khan et al.⁵³ demonstrated the upper convected Maxwell MHD micropolar fluid with the impact of Joule heating and thermal radiation utilizing a hyperbolic heat flux.

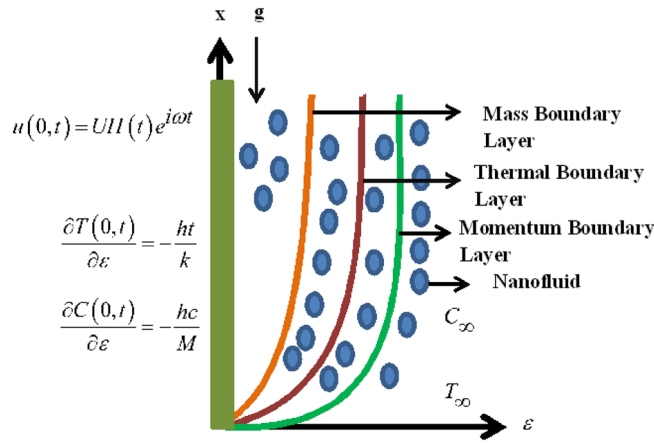


Figure 1. Sketch of the flow model.

To the best of author’s knowledge no one has consider the oscillating Maxwell nanofluid with the heat and mass transfer. So, motivated by this we study this problem analytically. The aim of this work is to explore oscillating Maxwell nanofluid with heat and mass transfer. The suspension of graphene nanoparticles and engine oil (base fluid) is taken in consideration. The governing equation is solved through LT. The solution for temperature, concentration and velocity are calculated analytically. Temperature slope and concentration gradient in the form of Nusslet number and Sherwood number are also acquired. Finally, the influence of various embedded factors on temperature, concentration and velocity shows graphically as well as theoretically.

Problem statement

Let us assume Maxwell nanofluid passed on an infinite oscillating vertical plate with heat and mass transfer. ε is perpendicular to the plate while plate along x -axis. Both the fluid and the plate are initially at rest with ambient temperature T_∞ and ambient concentration C_∞ . After some time at $t = 0^+$ the plate begins oscillation in its plane ($\varepsilon = 0$) as indicated with velocity $\underline{U}H(t)e^{i\omega t}$, where \underline{U} is the amplitude, ω represents the frequency of the oscillation of the plate, $H(t)$ is the unit step function and i is the unit vector in the vertical flow direction. Chemical reaction phenomenon is also incorporated to elaborate mass diffusion response. We suppose that the velocity, concentration and velocity is the function of ε and t . The governing equations is model in the following form. Figure 1 shows the geometry of the flow problem.

$$\rho_{nf} \left(1 + \lambda_0 \frac{\partial}{\partial t} \right) \frac{\partial u(\varepsilon, t)}{\partial t} = \mu_{nf} \frac{\partial^2 u(\varepsilon, t)}{\partial \varepsilon^2} + \left(1 + \lambda_0 \frac{\partial}{\partial t} \right) g(\rho\beta_t)_{nf} (T - T_\infty) + \left(1 + \lambda_0 \frac{\partial}{\partial t} \right) g(\rho\beta_m)_{nf} (C - C_\infty) \tag{1}$$

$$(\rho c_p)_{nf} \frac{\partial T(\varepsilon, t)}{\partial t} = k_{nf} \frac{\partial^2 T(\varepsilon, t)}{\partial \varepsilon^2} - \frac{\partial q_r}{\partial \varepsilon} \tag{2}$$

$$\frac{\partial C(\varepsilon, t)}{\partial t} = M \frac{\partial^2 C(\varepsilon, t)}{\partial \varepsilon^2} - K(C - C_\infty) \tag{3}$$

Here, ρ_{nf} is the density of nanofluid, λ_0 represents the Maxwell fluid parameter, μ_{nf} denotes the dynamic viscosity of nanofluid, g is the gravitational acceleration, $(\beta_t)_{nf}$ represents the coefficient of thermal expansion of nanofluid, c_p denotes the specific heat, $(\beta_m)_{nf}$ represents the coefficient of mass expansion of nanofluid, K represents the chemical reaction parameter, M_{nf} shows the diffusion species coefficient.

The corresponding initial conditions (ICs) and boundary conditions (BCs) are of the following form⁴⁹:

$$\begin{aligned} u(\varepsilon, 0) = 0, T(\varepsilon, 0) = T_\infty, C(\varepsilon, 0) = C_\infty, \\ u(0, t) = \underline{U}H(t)e^{i\omega t}, \frac{\partial T(0,t)}{\partial \varepsilon} = -\frac{ht}{k}, \frac{\partial C(0,t)}{\partial \varepsilon} = -\frac{hc}{M}, \varepsilon, t > 0 \\ u(\varepsilon, t) = 0, T(\varepsilon, t) = T_\infty, C(\varepsilon, t) = C_\infty \text{ as } \varepsilon \rightarrow \infty. \end{aligned} \tag{4}$$

where T_∞ is the ambient temperature, ht represents the coefficient of heat transfer, C_∞ demonstrates the ambient concentration, and hc shows the coefficient of mass transfer.

Using Rosseland approximations^{9,31,33} and gaining the small temperature variation between the temperature T_∞ of the free stream and the fluids temperature T , exploring the Taylor theorem on T^4 about T_∞ and omitting the numbers of 2nd and higher order, we get

$$q_r = -\frac{4\phi^*}{3\kappa^*} \frac{\partial T^4}{\partial \varepsilon} \tag{5}$$

Model	ρ (kg/m ³)	c_p (kJ/kg)	k (Wm ⁻¹ k ⁻¹)	$\beta \times 10^5$ k ⁻¹
Graphene	2250	2100	2500	21
Engine oil	884	1910	0.144	70

Table 1. Properties of nano particles.

and

$$T^4 \cong 4T_\infty^3 T - 3T_\infty^4 \tag{6}$$

where ϕ^*, κ^* are respectively Stefan boltzman constants, is the mean absorption coefficient. Substituting (5) into (2) we obtain the following form

$$(\rho c_p)_{nf} \frac{\partial T(\varepsilon, t)}{\partial t} = k_{nf} \frac{\partial^2 T(\varepsilon, t)}{\partial \varepsilon^2} + \frac{16\phi^* T_\infty^3}{3\kappa^*} \frac{\partial^2 T(\varepsilon, t)}{\partial \varepsilon^2} \tag{7}$$

The thermo-physical characteristics of nanoparticles were given by³⁵;

$$\begin{aligned} \rho_{nf} &= (1 - \vartheta)\rho_f + \vartheta\rho_s, \mu_{nf} = (1 - \vartheta)^{-2.5}\mu_f, (\rho\beta_t)_{nf} = (1 - \vartheta)(\rho\beta_t)_f + \vartheta(\rho\beta_t)_s, \\ (\rho\beta_m)_{nf} &= (1 - \vartheta)(\rho\beta_m)_f + \vartheta(\rho\beta_m)_s, (\rho c_p)_{nf} = (1 - \vartheta)(\rho c_p)_f + \vartheta(\rho c_p)_s, \\ \frac{k_{nf}}{k_f} &= \frac{(k_s + 2k_f) - 2\vartheta(k_f - k_s)}{(k_s - 2k_f) + \vartheta(k_f - k_s)}. \end{aligned}$$

The dimensionless parameters are given below;

$$\overset{\circ}{u} = \frac{u}{U}, \overset{\circ}{t} = \frac{U^2}{\nu} t, \overset{\circ}{\omega} = \frac{\nu}{U^2} \omega, \overset{\circ}{y} = \frac{y}{U}, \overset{\circ}{\lambda} = \frac{U^2}{\nu} \lambda_0 \tag{8}$$

After substituting the above dimensionless parameters in Eqs. (1), (3) and (7) we get these governing dimensionless equations and dropping the $\overset{\circ}$ from the above dimensionless factors,

$$\vartheta_1 \left(1 + \lambda \frac{\partial}{\partial t}\right) \frac{\partial u(\varepsilon, t)}{\partial t} = \vartheta_2 \frac{\partial u^2(\varepsilon, t)}{\partial \varepsilon^2} + \left(1 + \lambda \frac{\partial}{\partial t}\right) \vartheta_3 Gr_t \theta(\varepsilon, t) + \left(1 + \lambda \frac{\partial}{\partial t}\right) \vartheta_4 Gr_m \hat{C}(\varepsilon, t), \tag{9}$$

$$\vartheta_5 Pr \frac{\partial \theta(\varepsilon, t)}{\partial t} = \vartheta_6 (1 + Rd) \frac{\partial^2 \theta(\varepsilon, t)}{\partial \varepsilon^2}, \tag{10}$$

$$Sc \frac{\partial C(\varepsilon, t)}{\partial t} = \frac{\partial^2 C(\varepsilon, t)}{\partial \varepsilon^2} - ScKC(\varepsilon, t) \tag{11}$$

where

$$\begin{aligned} \theta &= \frac{Uk}{\nu ht} (T - T_\infty), Pr = \frac{\mu c_p}{k}, Gr_t = \left(\frac{\nu}{U^2}\right)^2 \frac{g\beta_t ht}{k}, Gr_m = \left(\frac{\nu}{U^2}\right)^2 \frac{g\beta_m hc}{M}, Sc = \frac{\nu}{M}, \\ Rd &= \frac{16\phi^* T_\infty^3}{3\kappa\kappa^*}, \hat{K} = \frac{\nu K}{U^2}, \hat{C} = \frac{UM}{\nu hc} (C - C_\infty), \vartheta_1 = (1 - \vartheta) + \vartheta \frac{\rho_s}{\rho_f}, \vartheta_2 = (1 - \vartheta)^{-2.5} \\ \vartheta_3 &= (1 - \vartheta) + \vartheta \frac{(\beta_t \rho)_s}{(\beta_t \rho)_f}, \vartheta_4 = (1 - \vartheta) + \vartheta \frac{(\beta_m \rho)_s}{(\beta_m \rho)_f}, \vartheta_5 = (1 - \vartheta) + \vartheta \frac{(c_p \rho)_s}{(c_p \rho)_f}, \vartheta_6 = \frac{k_{nf}}{k_f}. \end{aligned}$$

Here, θ denotes the dimensionless temperature, Pr shows Prandtl number, Gr_t demonstrates thermal Grashof number, Gr_m represents mass Grashof number, ϑ denotes volume fraction parameter and Sc represents Schmidt number.

The dimensionless ICs and BCs are as follow and skip $\overset{\circ}$ from the non-dimensional factors

$$\begin{aligned} u(\varepsilon, 0) &= 0, \theta(\varepsilon, 0) = 0, C(\varepsilon, 0) = 0 \\ u(0, t) &= H(t)e^{i\omega t}, \frac{\partial \theta(0, t)}{\partial \varepsilon} = -1, \frac{\partial C(0, t)}{\partial \varepsilon} = -1, \\ u(\varepsilon, t) &= 0, \theta(\varepsilon, t) = 0, C(\varepsilon, t) = 0, \varepsilon \rightarrow \infty. \end{aligned} \tag{12}$$

The thermo-physical property of graphene (nanoparticles) and engine oil (base fluid) are tabulated in table. 1

Problem solution

Temperature. Taking LT on Eq. (10) and also using the related ICs and BCs, we get the following transform form;

$$\bar{\theta}(\varepsilon, r) = \frac{1}{\sqrt{a_0 \text{Pr}_{eff}} r^{\frac{3}{2}}} e^{-\varepsilon \sqrt{a_0 \text{Pr}_{eff}} \cdot r}, \quad (13)$$

The inverse LT of Eq. (13) has the following final form,

$$\theta(\varepsilon, t) = \frac{2\sqrt{t}}{\sqrt{a_0 \text{Pr}_{eff}}} \left[\frac{1}{\sqrt{\pi}} e^{-\varepsilon \frac{a_0 \text{Pr}_{eff}}{4t}} - \varepsilon \frac{\sqrt{a_0 \text{Pr}_{eff}}}{2\sqrt{t}} \text{erfc} \left(\varepsilon \frac{\sqrt{a_0 \text{Pr}_{eff}}}{2\sqrt{t}} \right) \right]. \quad (14)$$

Nusslet number. The Nusslet number, measure the rate of heat transfer at the plate can be acquired by differentiating Eq. (13) with respect to ε and using $\varepsilon = 0$, we get the constant term. i.e.

$$Nu(t) = 1 \quad (15)$$

This shows the heat is transfer due to purely conduction.

Concentration. Applying LT on Eq. (11) and also utilizing the respective ICs and BCs, we acquire the following transform form;

$$\bar{C}(\varepsilon, r) = \frac{1}{r\sqrt{\text{Sc}(K+r)}} e^{-\varepsilon \sqrt{\text{Sc}(K+r)}} \quad (16)$$

The Laplace inverse transform of Eq. (16) as;

$$C(\varepsilon, t) = \frac{1}{2\sqrt{\text{Sc}K}} \left[e^{-\varepsilon \sqrt{\text{Sc}K}} \text{erfc} \left(\frac{\varepsilon \sqrt{\text{Sc}}}{2\sqrt{t}} - \sqrt{Kt} \right) - e^{-\varepsilon \sqrt{\text{Sc}K}} \text{erfc} \left(\frac{\varepsilon \sqrt{\text{Sc}}}{2\sqrt{t}} + \sqrt{Kt} \right) \right] \quad (17)$$

Sherwood number. The Sherwood number measure the mass transfer at the plate. The Sherwood number defined and represented by,

$$Sh = - \left(\frac{\partial C(\varepsilon, t)}{\partial \varepsilon} \right)_{\varepsilon=0} \quad (18)$$

Now to obtain Sherwood number we differentiate Eq. (16) with respect to ε and utilizing $\varepsilon = 0$, we get

$$Sh(t) = 1 \quad (19)$$

Velocity. The Laplace transform of Eq. (9) and also the appropriate ICs and BCs in Eq. (12) we get the following transform form;

$$\begin{aligned} \bar{u}(\varepsilon, r) = & \left[\frac{1}{r - i\omega} - \frac{a_2 Gr_t}{\sqrt{a_0 \text{Pr}_{eff}}} W_0(r) + \frac{a_3 Gr_m}{\sqrt{\text{Sc}}} W_{11}(r) W_3(r) \right] * W_4(\varepsilon, r) \\ & + \left[\frac{a_2 Gr_t}{\sqrt{a_0 \text{Pr}_{eff}}} W_0(r) \right] * W_5(\varepsilon, r) - \left[\frac{a_3 Gr_m}{\sqrt{\text{Sc}}} W_3(r) \right] * W_6(\varepsilon, r). \end{aligned} \quad (20)$$

Here,

$$W_0(r) = \left[\frac{b_1 - b_0}{b_1^2} \frac{1}{r^{\frac{3}{2}}} + \frac{b_0}{b_1} \frac{1}{r^{\frac{5}{2}}} \frac{b_0 - b_1}{b_1^2 b_{11}} \left(\frac{b_{11}}{\sqrt{r} (r - (\sqrt{b_{11}})^2)} \right) \right] \quad (21)$$

$$W_3(r) = W_1(r) - W_2(r) \quad (22)$$

$$W_1(r) = \frac{b_0}{b_2 - r(r + b_4)} \quad (23)$$

$$W_2(r) = \frac{r}{b_2 - r(r + b_4)} \quad (24)$$

$$W_4(\varepsilon, r) = e^{-\varepsilon\sqrt{\lambda a_1} \sqrt{\left(r + \frac{b_0}{2}\right)^2 - \left(\frac{b_0}{2}\right)^2}} \tag{25}$$

$$W_{51}(\varepsilon, r) = e^{-\varepsilon\sqrt{a_0 \text{Pr}_{eff}} \sqrt{r}} \tag{26}$$

$$W_6(\varepsilon, r) = \frac{e^{-\varepsilon\sqrt{\text{Sc}(\overline{K+r})}}}{r\sqrt{\overline{K+r}}} \tag{27}$$

$$W_{12}(r) = W_{11}(r)W_3(r) \tag{28}$$

The inverse LT of Eqs. (21)–(27), we obtain

$$W_0(t) = \left[\frac{b_1 - b_0}{b_1^2} 2\sqrt{\frac{t}{\pi}} + \frac{b_0}{b_1} \frac{4t}{3} \sqrt{\frac{t}{\pi}} + \frac{b_0 - b_1}{b_1^2 b_{11}} e^{b_{11}t} \text{erf}\left(\sqrt{b_{11}t}\right) \right] \tag{29}$$

$$W_1(t) = b_0 \left[\frac{e^{t\left(-\frac{b_4}{2} - \frac{1}{2}\sqrt{4b_2 + b_4^2}\right)} - e^{t\left(-\frac{b_4}{2} + \frac{1}{2}\sqrt{4b_2 + b_4^2}\right)}}{\sqrt{4b_2 + b_4^2}} \right] \tag{30}$$

$$W_{11}(t) = \frac{\text{Erf}\left(\sqrt{Kt}\right)}{\sqrt{K}} \tag{31}$$

$$W_2(t) = \left[\frac{b_4 e^{t\left(-\frac{b_4}{2} - \frac{1}{2}\sqrt{4b_2 + b_4^2}\right)} - b_4 e^{t\left(-\frac{b_4}{2} + \frac{1}{2}\sqrt{4b_2 + b_4^2}\right)} + \sqrt{4b_2 + b_4^2} e^{t\left(-\frac{b_4}{2} - \frac{1}{2}\sqrt{4b_2 + b_4^2}\right)} + \sqrt{4b_2 + b_4^2} e^{t\left(-\frac{b_4}{2} + \frac{1}{2}\sqrt{4b_2 + b_4^2}\right)}}{2\sqrt{4b_2 + b_4^2}} \right] \tag{32}$$

$$\begin{aligned} w_1(\varepsilon, t) &= \left[W_5(\varepsilon, t) + \frac{1}{2a_1\lambda} \int_0^t W_5(\varepsilon, p) \frac{p}{\sqrt{t^2 - p^2}} I_1\left(\frac{1}{2a_1\lambda} \sqrt{t^2 - p^2}\right) dp \right] e^{-\frac{1}{2a_1\lambda}t} \\ &= \frac{\varepsilon\sqrt{t}}{2t\sqrt{\pi t}} e^{\left(-\frac{\varepsilon^2 a_1 \lambda}{4t} - \frac{1}{2a_1\lambda}t\right)} + \frac{1}{2a_1\lambda} e^{-\frac{1}{2\lambda}t} \\ &\quad \int_0^t \frac{\varepsilon\sqrt{a_1\lambda}}{2z\sqrt{\pi p}} e^{\left(-\frac{\varepsilon^2 a_1 \lambda}{4p}\right)} \frac{p}{\sqrt{t^2 - p^2}} I_1\left(\frac{1}{2a_1\lambda} \sqrt{t^2 - p^2}\right) dp, \end{aligned} \tag{33}$$

$$W_4(\varepsilon, t) = L^{-1}\{W_4(\varepsilon, r)\} = \begin{cases} w_1(\varepsilon, t); & \varepsilon > 0 \\ \delta(t); & \varepsilon = 0 \end{cases} \tag{34}$$

$$W_5(\varepsilon, t) = L^{-1}\{W_{51}(\varepsilon, r)\} = \begin{cases} \frac{\varepsilon\sqrt{a_0 \text{Pr}_{eff}} e^{-\varepsilon^2 \frac{a_0 \text{Pr}_{eff}}{4t}}}{2t\sqrt{\pi t}}; & \varepsilon > 0 \\ \delta(t); & \varepsilon = 0. \end{cases} \tag{35}$$

$$W_6(\varepsilon, t) = \frac{1}{2\sqrt{K}} \left[e^{-\varepsilon\sqrt{\text{Sc}K}} \text{erfc}\left(\frac{\varepsilon\sqrt{\text{Sc}}}{2\sqrt{t}} - \sqrt{Kt}\right) - e^{-\varepsilon\sqrt{\text{Sc}K}} \text{erfc}\left(\frac{\varepsilon\sqrt{\text{Sc}}}{2\sqrt{t}} + \sqrt{Kt}\right) \right] \tag{36}$$

The Laplace inverse transform of Eq. (20) and utilizing the Faltung theorem, we get

$$\begin{aligned} u(\varepsilon, t) &= \int_0^t e^{i\omega(t-v)} W_4(\varepsilon, v) dv - \frac{a_2 Gr_t}{\sqrt{a_0 \text{Pr}_{eff}}} \int_0^t W_0(t-v) W_4(\varepsilon, v) dv + \frac{a_3 Gr_m}{\sqrt{\text{Sc}}} \int_0^t W_{12}(t-v) W_4(\varepsilon, v) dv \\ &\quad + \frac{a_2 Gr_t}{\sqrt{a_0 \text{Pr}_{eff}}} \int_0^t W_0(t-v) W_5(\varepsilon, v) dv - \frac{a_3 Gr_m}{\sqrt{\text{Sc}}} \int_0^t W_3(t-v) W_6(\varepsilon, v) dv \end{aligned} \tag{37}$$

Special cases

In the absence of nanoparticles, we obtained the solution of Fetecau et al.³³

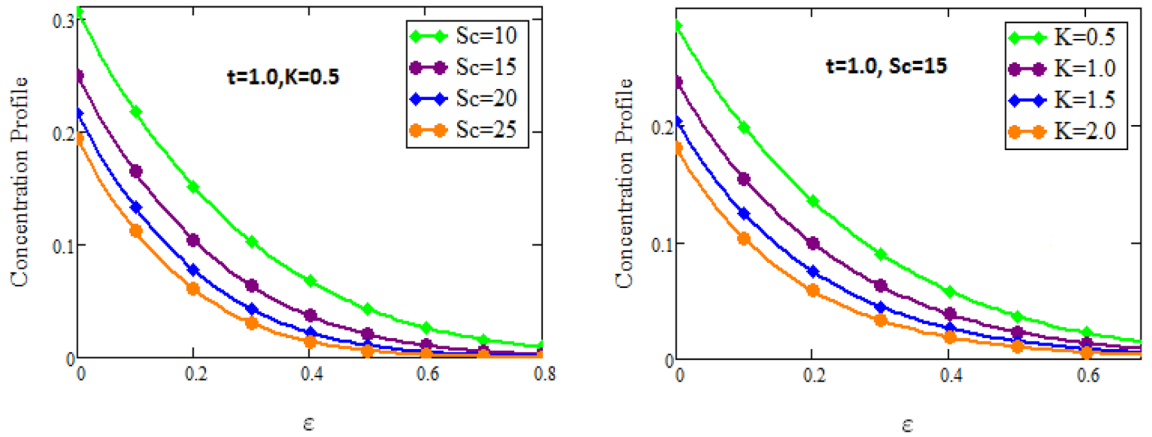


Figure 2. Concentration curves for various values of Sc and K .

$$\theta(\varepsilon, t) = \frac{2\sqrt{t}}{\sqrt{\text{Pr}_{eff}}} \left[\frac{1}{\sqrt{\pi}} e^{-\varepsilon \frac{\text{Pr}_{eff}}{4t}} - \varepsilon \frac{\sqrt{\text{Pr}_{eff}}}{2\sqrt{t}} \text{erfc} \left(\varepsilon \frac{\sqrt{\text{Pr}_{eff}}}{2\sqrt{t}} \right) \right]. \tag{38}$$

When we put $K = 0$ and $Sc = 1$ in Eq. (11), we get the solution in the form of as given under:

$$C(\varepsilon, t) = \sqrt{\frac{4t}{\pi}} e^{-\frac{\varepsilon^2}{4t}} - \varepsilon \text{erfc} \left(\frac{\varepsilon}{2\sqrt{t}} \right) \tag{39}$$

In the absence of Maxwell fluid coefficient (Newtonian fluid $\lambda = 0$) in Eq. (9), we acquired the following solution:

$$\begin{aligned} u(\varepsilon, t) = & \int_0^t e^{i\omega(t-v)} W_{13}(\varepsilon, v) dv - \frac{a_2 Gr_t}{(a_0 \text{Pr}_{eff} - a_1) \sqrt{a_0 \text{Pr}_{eff}}} \left(\frac{e^{-\frac{\varepsilon^2}{4t}} \sqrt{t} (4t + \varepsilon^2)}{3\sqrt{\pi}} - \frac{1}{6} (6t\varepsilon + \varepsilon^3) \text{erfc} \left(\frac{\varepsilon}{2\sqrt{t}} \right) \right) \\ & + \frac{a_3 Gr_m}{\sqrt{Sc}} \int_0^t \frac{e^{-\frac{m_1}{m_2}(t-v)}}{m_2} W_{14}(\varepsilon, v) dv + \frac{a_2 Gr_t}{(a_0 \text{Pr}_{eff} - a_1) \sqrt{a_0 \text{Pr}_{eff}}} \left(\frac{e^{-\frac{a_0 \text{Pr}_{eff} \varepsilon^2}{4t}} \sqrt{t} (4t + a_0 \text{Pr}_{eff} \varepsilon^2)}{3\sqrt{\pi}} \right) \\ & - \frac{a_2 Gr_t}{(a_0 \text{Pr}_{eff} - a_1) \sqrt{a_0 \text{Pr}_{eff}}} \left(\frac{1}{6} \left(6t \sqrt{a_0 \text{Pr}_{eff}} \varepsilon + \left(\sqrt{a_0 \text{Pr}_{eff}} \varepsilon \right)^3 \right) \text{erfc} \left(\frac{\sqrt{a_0 \text{Pr}_{eff}} \varepsilon}{2\sqrt{t}} \right) \right) - \frac{a_3 Gr_m}{\sqrt{Sc}} \int_0^t \frac{e^{-\frac{m_1}{m_2}(t-v)}}{m_2} W_6(\varepsilon, v) dv \end{aligned} \tag{40}$$

where

$$W_{13}(\varepsilon, t) = \begin{cases} \frac{e^{-\frac{\varepsilon^2}{4t}} \varepsilon}{2\sqrt{\pi t^{\frac{3}{2}}}}, & \varepsilon > 0, \\ W_{14}(\varepsilon, t) = \frac{ie^{-Kt}}{2} \left[e^{i\varepsilon\sqrt{K}} \text{erfc} \left\{ \frac{\varepsilon}{2\sqrt{t}} + i\sqrt{Kt} \right\} - e^{-i\varepsilon\sqrt{K}} \text{erfc} \left\{ \frac{\varepsilon}{2\sqrt{t}} - i\sqrt{Kt} \right\} \right] \end{cases}$$

Numerical results and discussion

In order to see the physical meaning of the problem, we use the LT method to obtain the solution for temperature, concentration, velocity, rate of heat transfer and rate of mass transfer. These solutions have been studied graphically by giving numerical values to various embedded parameters like radiation factor, chemical reaction factor, thermal Grashof number, mass Grashof number, Maxwell fluid coefficient, Schmidt number, Prandtl number. The value of volume fraction parameter is taken 0.01.

Figure 2 characterizes the concentration for variations of Schmidt number Sc and chemical reaction factor K . It is found that by increasing the value of Schmidt number Sc and chemical reaction factor K , the concentration of the nanofluid decreases. Physically, there is inverse relation between Schmidt number and mass diffusivity. As we enhance Schmidt number Sc , the mass diffusion is de-escalates. Thus, concentration profile decreases. Similarly, concentration profile decreases with the increasing estimation of chemical reaction factor K . This behavior is due to less fluid particles are produced as a product. In Fig. 3 the flow profile of Maxwell fluid is studied under the revamping of thermal Grashof number for both the sine and cosine oscillations. The velocity distribution for both sine and cosine oscillation is the growing function as we grow the value of thermal Grashof number Gr_t . Physically, this characteristic is because of the viscous and thermal buoyancy forces in flow of fluid. The greater the value of Gr_t shows the fluid is heated that bolsters the impact of thermal buoyancy forces because of the existence of convection currents. These currents get the value of great importance due to prevailing temperature slop and eventually cause the viscous forces to sink. As a result, the fluid's velocity enhances. Figure 4 displays the impact of mass Grashof number on velocity. It is also have same behavior like Fig. 3 i.e. the

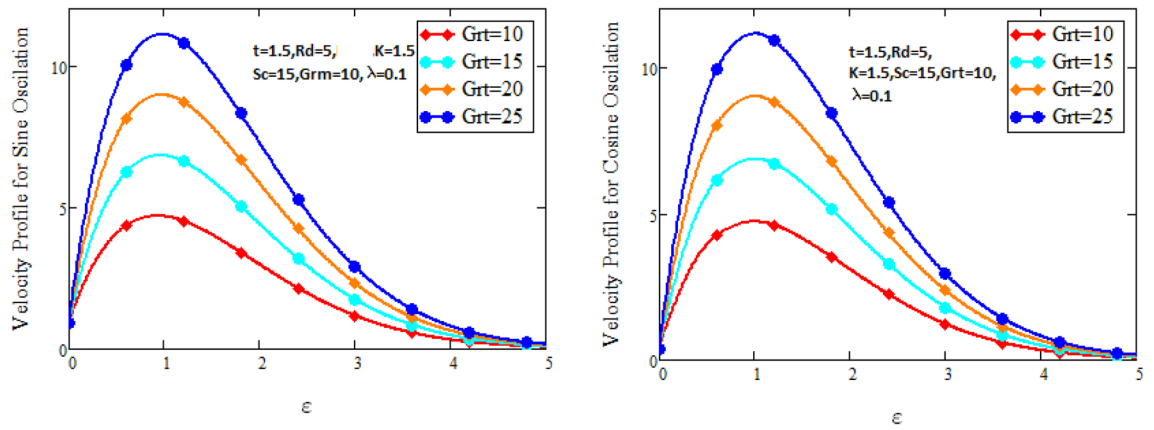


Figure 3. Velocity curves for various values of Gr_t .

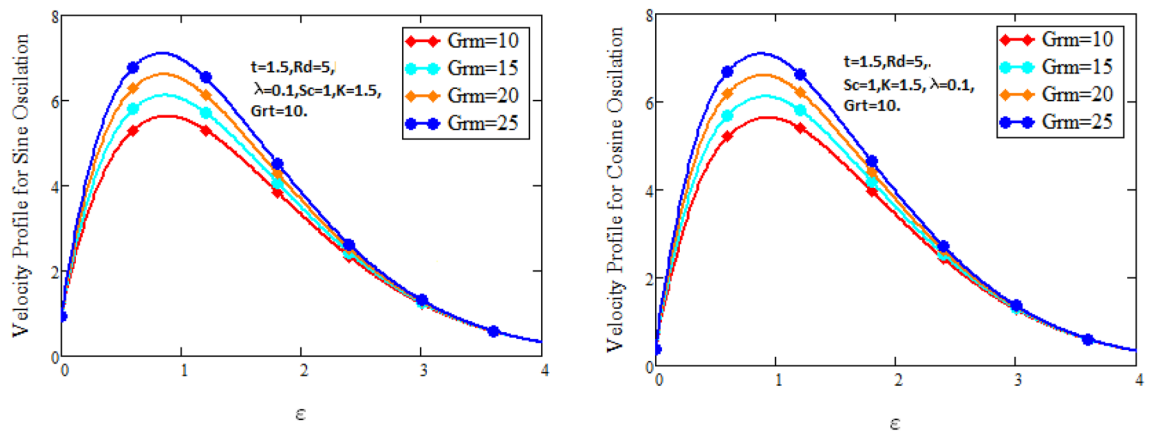


Figure 4. Velocity curves for various values of Gr_m .

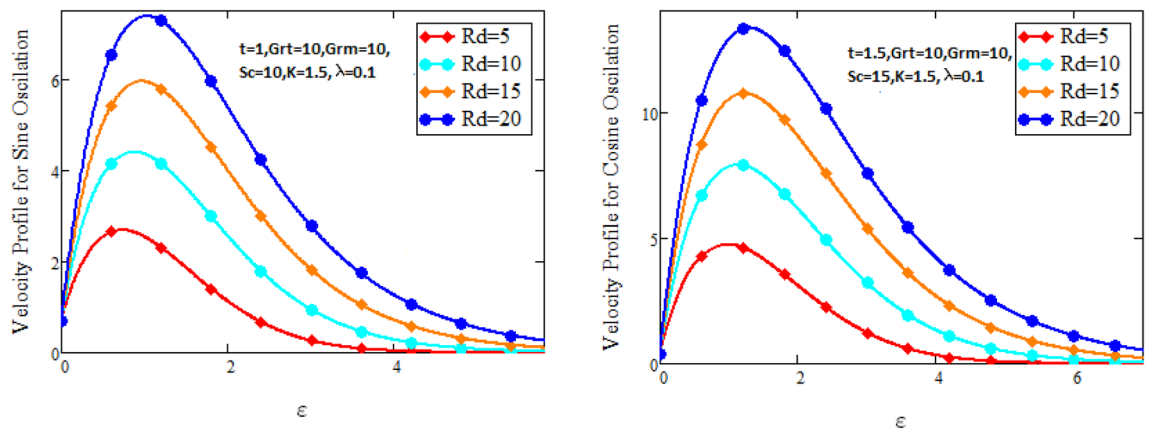


Figure 5. Velocity curves for various values of Rd .

enhancement of Gr_m enhances the velocity of the fluid. This is due to the enhancement in mass buoyancy force and buoyancy force enhances concentration gradient, which result enhances the velocity. Figure 5 portrays the behavior of radiation coefficient Rd for both sine and cosine oscillation. It characterize that the fluid's velocity accelerated with the greater value of Rd . Physically, rate of energy transfer explains this increase. As Rd increments, rate of energy transfer to the fluids grows which results to weak the bond between fluid particles. As a result these poorly associated particles collectively give much weaker viscosity to fluid motion and gradually fluid gets accelerated. Figure 6 shows the relationship between Schmidt number and velocity of the fluid. It is spotted that the increases in Schmidt number decelerate the fluid's velocity for both the oscillations. Physically,

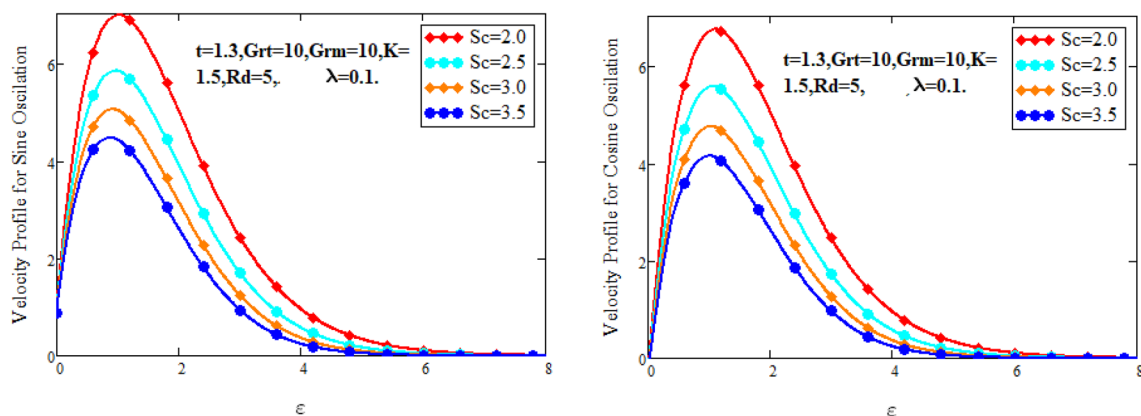


Figure 6. Velocity curves for various values of Sc .

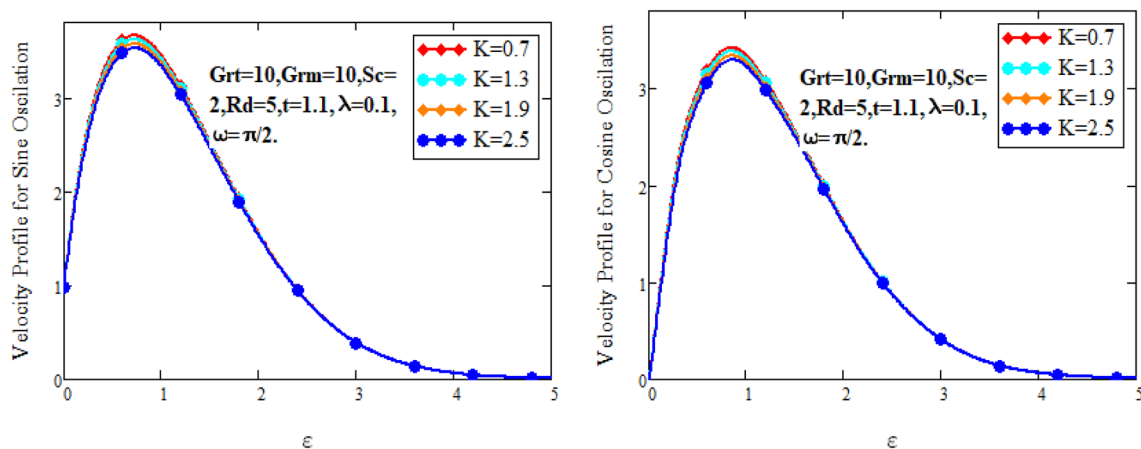


Figure 7. Velocity curves for various values of K .

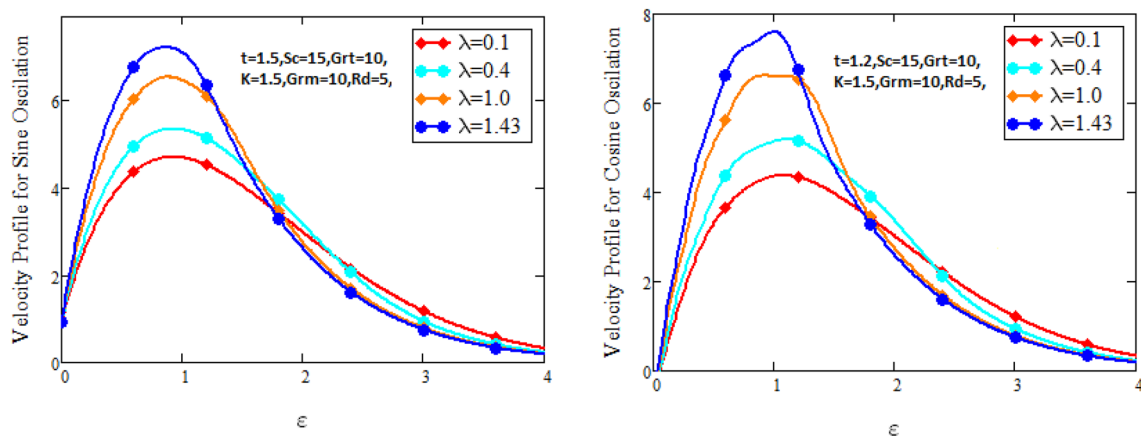


Figure 8. Velocity curves for various values of λ .

as Schmidt number Sc increases, the molecular diffusivity reduces due to which velocity decreases. Figure 7 exhibits the effects of chemical reaction factor on velocity distribution for both the sine and cosine oscillation. Clearly Fig. 7 demonstrates the de-escalation in fluid velocity as we grow the value of chemical reaction factor. The variation of velocity distribution because of Maxwell fluid coefficient λ for both the oscillation is described in Fig. 8. It is realized the fluid flow is increasing function for greater value of λ . Physically, this observation is because of the retard in boundary layer thickness. Velocity shows the significant behavior in the main stream region and finally approaching to zero.

Figure 9 shows the behavior of graphene nanoparticle on velocity profile. It can be seen that the velocity of nanofluid reduces for the growing value of volume fraction. This is because of increases the nanoparticles makes denser the fluid, so its velocity decelerates.

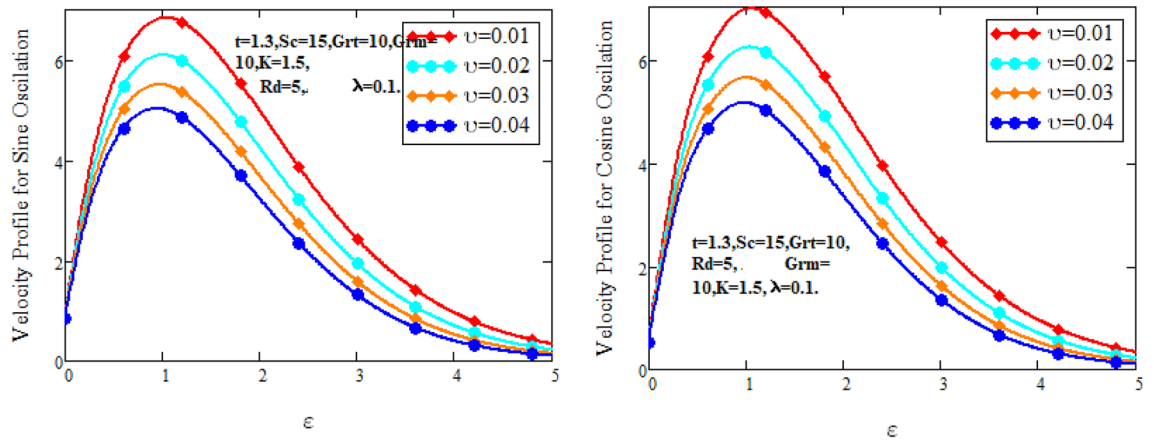


Figure 9. Velocity curves for various values of ϑ .

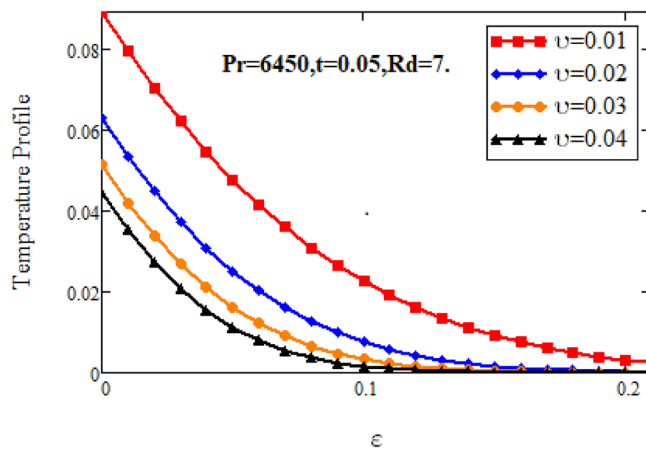


Figure 10. Temperature profiles for various values of ϑ .

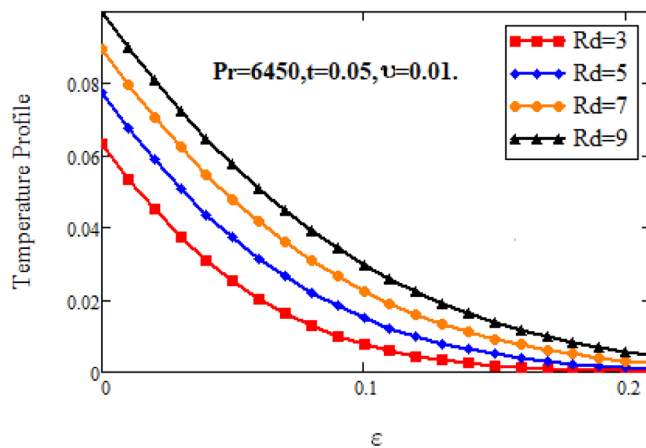


Figure 11. Temperature profiles for various values of Rd .

Figures 10 and 11 highlight the impact of various parameters on temperature profile of nano fluid. Figure 10 depicts the influence of volume fraction on temperature profile of nanofluid. It is observed that the temperature of nanofluid decelerates with accelerating the estimations of volume factor. Physically, this behavior is due to decrease of thermal conductivity on adding nanoparticles, which results decelerates the temperature of nanofluid. Figure 11 shows the increase in nanofluid’s temperature with increasing radiation parameter. Since increase in at fixed value of and, decelerates the value of, therefore slop of radioactive heat flux increases which lead to grow

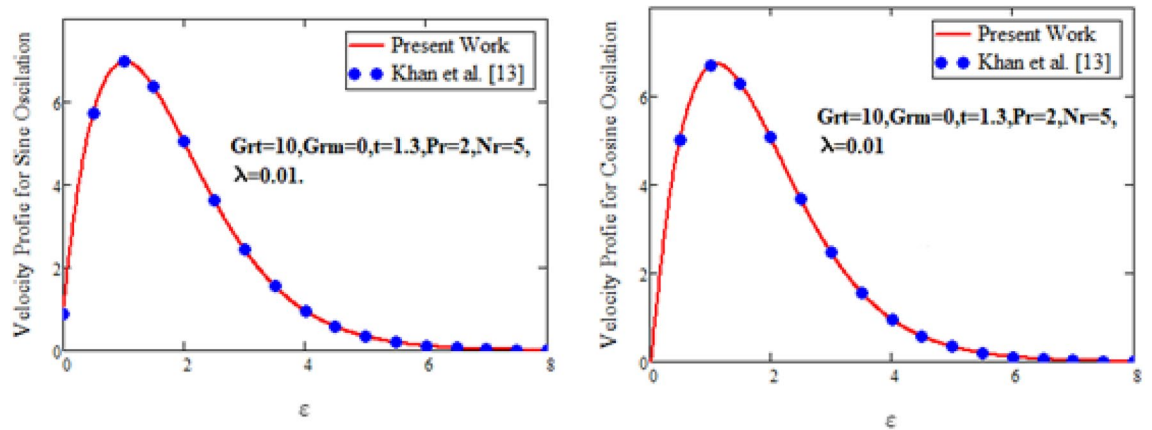


Figure 12. Comparative study of velocity profiles.

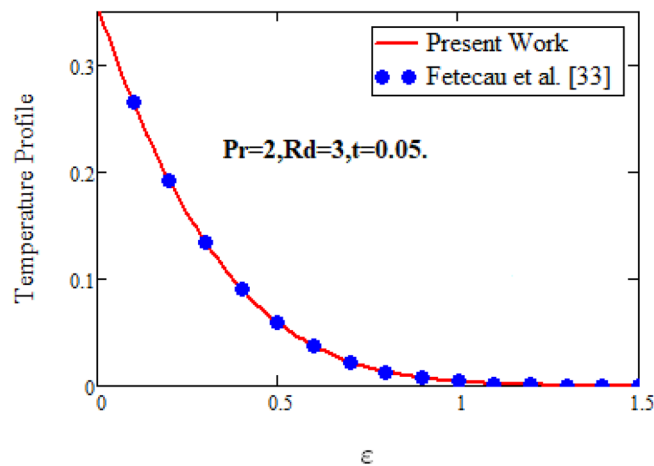


Figure 13. Comparative study of temperature profiles.

the radiative heat transfer rate and gradually the fluid's temperature increments, It means that thickness of energy boundary layer reduces and temperature is distributed more uniformly.

In order to authenticate our present solutions, Figs. 12 and 13, are presented. It can be observed if the volume fraction parameter ϑ are removed from temperature field and ϑ and Gr_m are deleting from the velocity field of the current model, then the present solutions for temperature and velocity field are in excellent agreement with the velocity solution of ordinary Maxwell fluid model of Khan et al.¹³ for both sine and cosine oscillations and the temperature solution of Fetecau et al.³³.

Conclusion

The aspiration of this work was to evaluate the oscillating Maxwell nanofluid with heat and mass transfer. The analytical solution for temperature, concentration, and velocity were obtained through LT method. The rate of heat and mass transfer was also measured in the form of Nusslet number and Sherwood number. Finally, the effect of different physical factors were shown in discussion section graphically and theoretically for both sine and cosine oscillation. The solution of Newtonian fluid was also analyzed as a special case. Following are the key concepts of this work (Supplementary Information S1):

- The concentration profile is decreasing function for Schmidt number Sc .
- Decrease occurs in concentration with increasing the estimation of chemical reaction factor K .
- The velocity of the nanofluid grows, when thermal Grashof number Gr_t is accelerated.
- The nanofluid's velocity enhances with the enhancement of mass Grashof number Gr_m .
- The velocity field is accelerated as we accelerate the estimation of Maxwell fluid parameter λ .
- Reduction occurs in velocity with higher value of Schmidt number Sc .
- The nanofluid's velocity is increasing function as we increase the value of radiation parameter Rd while decreasing function against the chemical reaction factor K .
- Volume function also reduces the nanofluid's velocity.

- The temperature of fluid is growing function when radiation parameter Rd is increases, while falls when volume fraction parameter ϑ enlarges.
- Nusslet number and Sherwood number are constant.

Data availability

All data generated or analyzed during this study are included in this article.

Received: 21 March 2022; Accepted: 11 July 2022

Published online: 16 July 2022

References

- Hoyt, J. W. Some applications of non-newtonian fluid flow. In *Rheology Series* (Vol. 8, pp. 797–826). Elsevier (1999).
- Pérez-Reyes, I., Vargas-Aguilar, R. O., Pérez-Vega, S. B., & Ortiz-Pérez, A. S. Applications of viscoelastic fluids involving hydrodynamic stability and heat transfer. *Polym. Rheol.*, 29 (2018).
- Sheikholeslami, M., Hayat, T. & Alsaedi, A. MHD free convection of Al₂O₃–water nanofluid considering thermal radiation: A numerical study. *Int. J. Heat Mass Transf.* **96**, 513–524 (2016).
- Sheikholeslami, M. & Ganji, D. D. CVFEM for free convective heat transfer of CuO-water nanofluid in a tilted semi annulus. *Alex. Eng. J.* **56**(4), 635–645 (2017).
- Sheikholeslami, M. & Rashidi, M. M. Effect of space dependent magnetic field on free convection of Fe₃O₄–water nanofluid. *J. Taiwan Inst. Chem. Eng.* **56**, 6–15 (2015).
- Sheikholeslami, M., Vajravelu, K. & Rashidi, M. M. Forced convection heat transfer in a semi annulus under the influence of a variable magnetic field. *Int. J. Heat Mass Transf.* **92**, 339–348 (2016).
- Riaz, M. B., Atangana, A., & Iftikhar, N. Heat and mass transfer in Maxwell fluid in view of local and non-local differential operators. *J. Therm. Anal. Calorimetry* **143**(6) (2021).
- Riaz, M. B. & Iftikhar, N. A comparative study of heat transfer analysis of MHD Maxwell fluid in view of local and nonlocal differential operators. *Chaos, Solitons Fractals* **132**, 109556 (2020).
- Jamil, B., Anwar, M. S., Rasheed, A. & Irfan, M. MHD Maxwell flow modeled by fractional derivatives with chemical reaction and thermal radiation. *Chin. J. Phys.* **67**, 512–533 (2020).
- Haque, E. U., Awan, A. U., Raza, N., Abdullah, M. & Chaudhry, M. A. A computational approach for the unsteady flow of Maxwell fluid with Caputo fractional derivatives. *Alex. Eng. J.* **57**(4), 2601–2608 (2018).
- Na, W., Shah, N. A., Tlili, I. & Siddique, I. Maxwell fluid flow between vertical plates with damped shear and thermal flux: free convection. *Chin. J. Phys.* **65**, 367–376 (2020).
- Khan, I., Shah, N. A. & Dennis, L. C. C. A scientific report on heat transfer analysis in mixed convection flow of Maxwell fluid over an oscillating vertical plate. *Sci. Rep.* **7**(1), 1–11 (2017).
- Khan, I., Shah, N. A., Mahsud, Y. & Vieru, D. Heat transfer analysis in a Maxwell fluid over an oscillating vertical plate using fractional Caputo-Fabrizio derivatives. *Eur. Phys. J. Plus* **132**(4), 1–12 (2017).
- Abro, K. A., & Shaikh, A. A. (2015). Exact analytical solutions for Maxwell fluid over an oscillating plane. *Sci. Int.(Lahore) ISSN*, 27, 923–929.
- Kumar, M. S., Sandeep, N., Kumar, B. R. & Saleem, S. A comparative study of chemically reacting 2D flow of Casson and Maxwell fluids. *Alex. Eng. J.* **57**(3), 2027–2034 (2018).
- Ahmed, T. N. & Khan, I. Mixed convection flow of sodium alginate (SA-NaAlg) based molybdenum disulphide (MoS₂) nanofluids: Maxwell Garnetts and Brinkman models. *Res. Phys.* **8**, 752–757 (2018).
- Farooq, A. *et al.* On the flow of MHD generalized maxwell fluid via porous rectangular duct. *Open Phys.* **18**(1), 989–1002 (2020).
- Khan, I., Ali, F. & Shafie, S. Exact Solutions for Unsteady Magnetohydrodynamic oscillatory flow of a maxwell fluid in a porous medium. *Zeitschrift für Naturforschung A* **68**(10–11), 635–645 (2013).
- Zheng, L., Zhao, F. & Zhang, X. Exact solutions for generalized Maxwell fluid flow due to oscillatory and constantly accelerating plate. *Nonlinear Anal. Real World Appl.* **11**(5), 3744–3751 (2010).
- Sandeep, N. & Sulochana, C. Momentum and heat transfer behaviour of Jeffrey, Maxwell and Oldroyd-B nanofluids past a stretching surface with non-uniform heat source/sink. *Ain Shams Eng. J.* **9**(4), 517–524 (2018).
- Aman, S., Al-Mdallal, Q. & Khan, I. Heat transfer and second order slip effect on MHD flow of fractional Maxwell fluid in a porous medium. *J. King Saud Univ. Sci.* **32**(1), 450–458 (2020).
- Fetecau, C., Jamil, M., Fetecau, C. & Siddique, I. A note on the second problem of Stokes for Maxwell fluids. *Int. J. Non-Linear Mech.* **44**(10), 1085–1090 (2009).
- Shateyi, S. A new numerical approach to MHD flow of a Maxwell fluid past a vertical stretching sheet in the presence of thermophoresis and chemical reaction. *Bound. Value Probl.* **2013**(1), 1–14 (2013).
- Shah, N. A., Zafar, A. A. & Akhtar, S. General solution for MHD-free convection flow over a vertical plate with ramped wall temperature and chemical reaction. *Arab. J. Math.* **7**(1), 49–60 (2018).
- Fetecau, C., Shah, N. A. & Vieru, D. General solutions for hydromagnetic free convection flow over an infinite plate with Newtonian heating, mass diffusion and chemical reaction. *Commun. Theor. Phys.* **68**(6), 768 (2017).
- Seth, G. S., Hussain, S. M. & Sarkar, S. Hydromagnetic natural convection flow with heat and mass transfer of a chemically reacting and heat absorbing fluid past an accelerated moving vertical plate with ramped temperature and ramped surface concentration through a porous medium. *J. Egypt. Math. Soc.* **23**(1), 197–207 (2015).
- Singh, K. D., & Kumar, R. Fluctuating heat and mass transfer on unsteady MHD free convection flow of radiating and reacting fluid past a vertical porous plate in slip-flow regime (2011).
- Narahari, M., Bég, O. A., & Ghosh, S. K. Mathematical modelling of mass transfer and free convection current effects on unsteady viscous flow with ramped wall temperature (2011).
- Rajput, U. S., & Kumar, S. Radiation effects on MHD flow past an impulsively started vertical plate with variable heat and mass transfer. *Int. J. Appl. Math. Mech.* **8**(1), 66–85 (2012).
- Pattnaik, J. R., Dash, G. C. & Singh, S. Radiation and mass transfer effects on MHD flow through porous medium past an exponentially accelerated inclined plate with variable temperature. *Ain Shams Eng. J.* **8**(1), 67–75 (2017).
- Seth, G. S., Kumbhakar, B. & Sarkar, S. Soret and Hall effects on unsteady MHD free convection flow of radiating and chemically reactive fluid past a moving vertical plate with ramped temperature in rotating system. *Int. J. Eng. Sci. Technol.* **7**(2), 94–108 (2015).
- Kumam, P., Tassaddiq, A., Watthayu, W., Shah, Z., & Anwar, T. Modeling and simulation based investigation of unsteady MHD radiative flow of rate type fluid; a comparative fractional analysis. *Math. Comput. Simul.* (2021).
- Fetecau, C., Khan, I., Ali, F. & Shafie, S. Radiation and porosity effects on the magnetohydrodynamic flow past an oscillating vertical plate with uniform heat flux. *Zeitschrift für Naturforschung A* **67**(10–11), 572–580 (2012).

34. Tang, R., Rehman, S., Farooq, A., Kamran, M., Qureshi, M. I., Fahad, A., & Liu, J. B. A comparative study of natural convection flow of fractional maxwell fluid with uniform heat flux and radiation. *Complexity* (2021).
35. Aman, S., Salleh, M. Z., Ismail, Z., & Khan, I. Exact solution for heat transfer free convection flow of Maxwell nanofluids with graphene nanoparticles. *J. Phys. Conf. Ser.* **890**(1): 012004 (2017).
36. Murtaza, S., Iftekhar, M., Ali, F. & Khan, I. Exact analysis of non-linear electro-osmotic flow of generalized maxwell nanofluid: applications in concrete based nano-materials. *IEEE Access* **8**, 96738–96747 (2020).
37. Ali, R., Asjad, M. I., Aldalbahi, A., Rahimi-Gorji, M. & Rahaman, M. Convective flow of a Maxwell hybrid nanofluid due to pressure gradient in a channel. *J. Therm. Anal. Calorim.* **143**(2), 1319–1329 (2021).
38. Chu, Y. M., Ali, R., Asjad, M. I., Ahmadian, A. & Senu, N. Heat transfer flow of Maxwell hybrid nanofluids due to pressure gradient into rectangular region. *Sci. Rep.* **10**(1), 1–18 (2020).
39. Asjad, M. I., Ali, R., Iqbal, A., Muhammad, T. & Chu, Y. M. Application of water based drilling clay-nanoparticles in heat transfer of fractional Maxwell fluid over an infinite flat surface. *Sci. Rep.* **11**(1), 1–14 (2021).
40. Wang, F. *et al.* Comparative study of heat and mass transfer of generalized MHD Oldroyd-B bio-nano fluid in a permeable medium with ramped conditions. *Sci. Rep.* **11**(1), 1–32 (2021).
41. Arif, M., Kumam, P., Khan, D. & Wathayay, W. Thermal performance of GO-MoS₂/engine oil as Maxwell hybrid nanofluid flow with heat transfer in oscillating vertical cylinder. *Case Stud. Thermal Eng.* **27**, 101290 (2021).
42. Kumar, R. N. *et al.* Impact of magnetic dipole on thermophoretic particle deposition in the flow of Maxwell fluid over a stretching sheet. *J. Mol. Liq.* **334**, 116494 (2021).
43. Prasannakumara, B. C. Numerical simulation of heat transport in Maxwell nanofluid flow over a stretching sheet considering magnetic dipole effect. *Partial Differ. Equ. Appl. Math.* **4**, 100064 (2021).
44. Gowda, R. J., Rauf, A., Naveen Kumar, R., Prasannakumara, B. C. & Shehzad, S. A. Slip flow of Casson–Maxwell nanofluid confined through stretchable disks. *Indian J. Phys.* **1**, 1–9 (2021).
45. Kumar, V. *et al.* Analysis of single and multi-wall carbon nanotubes (SWCNT/MWCNT) in the flow of Maxwell nanofluid with the impact of magnetic dipole. *Comput. Theor. Chem.* **1200**, 113223 (2021).
46. Mabood, F., Rauf, A., Prasannakumara, B. C., Izadi, M. & Shehzad, S. A. Impacts of Stefan blowing and mass convection on flow of Maxwell nanofluid of variable thermal conductivity about a rotating disk. *Chin. J. Phys.* **71**, 260–272 (2021).
47. Li, Y. X. *et al.* Dual branch solutions (multi-solutions) for nonlinear radiative Falkner–Skan flow of Maxwell nanomaterials with heat and mass transfer over a static/moving wedge. *Int. J. Mod. Phys. C (IJMPC)* **32**(10), 1–20 (2021).
48. Gireesha, B. J., Prasannakumara, B. C., Umshaiah, M. & Shashikumar, N. S. Three dimensional boundary layer flow of MHD Maxwell nanofluid over a non-linearly stretching sheet with nonlinear thermal radiation. *J. Appl. Nonlinear Dyn.* **10**(02), 263–277 (2021).
49. Raza, N. & Ullah, M. A. A comparative study of heat transfer analysis of fractional Maxwell fluid by using Caputo and Caputo–Fabrizio derivatives. *Can. J. Phys.* **98**(1), 89–101 (2020).
50. Cheng, L. *et al.* Flow and heat transfer analysis of elastoviscoplastic generalized non-Newtonian fluid with hybrid nano structures and dust particles. *Int. Commun. Heat Mass Transfer* **126**, 105275 (2021).
51. Kameez, H., Alebraheem, J., Elmoasry, A., Saif, R. S. & Nawaz, M. Numerical investigation on transport of momenta and energy in micropolar fluid suspended with dusty, mono and hybrid nano-structures. *AIP Adv.* **10**(4), 045120 (2020).
52. Kameez, H., Nawaz, M. & Elmasry, Y. Role of hybrid nanostructures and dust particles on transport of heat energy in micropolar fluid with memory effects. *J. Thermal Anal. Calorimetry* **1**, 1–14 (2020).
53. Khan, S. M., Hammad, M., Batool, S. & Kameez, H. Investigation of MHD effects and heat transfer for the upper-convected Maxwell (UCM-M) micropolar fluid with Joule heating and thermal radiation using a hyperbolic heat flux equation. *Eur. Phys. J. Plus* **132**(4), 1–12 (2017).

Acknowledgements

Abdulaziz N. Alharbi would like to acknowledge the financial support of Taif University Researchers Supporting Project number (TURSP-2020/319), Taif University, Taif, Saudi Arabia.

Author contributions

Conceptualization, I.K. and T.B.; data curation, I.K.; funding acquisition, A.A.; methodology, M.K.; project administration, A.A. and M.K.; resources, S.R., M.K.; software, S.R. and A.F.; supervision, S.R., M.K. and A.F.; validation, A.F.; visualization, S.R. and A.F.; writing—original draft, S.R.; writing—review and editing, A.A., T.B. and A.F. All authors have read and agreed to the published version of the manuscript.

Competing interests

The authors declare no competing interests.

Additional information

Supplementary Information The online version contains supplementary material available at <https://doi.org/10.1038/s41598-022-16503-w>.

Correspondence and requests for materials should be addressed to T.B.

Reprints and permissions information is available at www.nature.com/reprints.

Publisher's note Springer Nature remains neutral with regard to jurisdictional claims in published maps and institutional affiliations.



Open Access This article is licensed under a Creative Commons Attribution 4.0 International License, which permits use, sharing, adaptation, distribution and reproduction in any medium or format, as long as you give appropriate credit to the original author(s) and the source, provide a link to the Creative Commons licence, and indicate if changes were made. The images or other third party material in this article are included in the article's Creative Commons licence, unless indicated otherwise in a credit line to the material. If material is not included in the article's Creative Commons licence and your intended use is not permitted by statutory regulation or exceeds the permitted use, you will need to obtain permission directly from the copyright holder. To view a copy of this licence, visit <http://creativecommons.org/licenses/by/4.0/>.

© The Author(s) 2022, corrected publication 2022